Structure and Intramolecular Charge-Transfer Dynamics of *p*-(Dimethylamino)benzonitrile in Solvent Clusters

Hiroyuki Saigusa,* Eijiro Iwase, and Masashi Nishimura

The Graduate School of Integrated Science, Yokohama City University, Yokohama 236-0027, Japan

Received: January 10, 2003; In Final Form: April 11, 2003

Excited-state dynamics of *p*-(dimethylamino)benzonitrile (DMABN) complexed with water and acetonitrile, DMABN$(H_2O)_n$ and DMABN(acetonitrile)$_n$, have been investigated as a function of cluster size by the spectroscopic techniques of resonant two-photon ionization, fluorescence excitation, dispersed fluorescence, and hole-burning. In water clusters, a distinct red shift of fluorescence is observed to occur for $n = 3$. A hole-burning measurement reveals that this behavior is strongly dependent on the excess vibrational energy deposited on the cluster, thereby suggesting the occurrence of intramolecular charge transfer (CT). However, the extent of the CT stabilization, which is manifested as the fluorescence red shift, is found to be much less than in bulk water. As the solvation number increases up to $n \approx 30$, the red shift appears to saturate and does not converge to the bulk limit. Similar saturation behavior is observed for acetonitrile clusters. The absence of bulklike CT emissions in both solvent clusters is attributed to their low internal temperatures or cluster rigidity, which impede large structural changes of the DMABN solute leading to CT. This cluster rigidity scenario suggests that the fluorescence from larger clusters originates from an unrelaxed CT state trapped in a solvent cage and thus further stabilization can be activated upon increasing cluster internal energy.

Introduction

The excited-state charge-transfer (CT) reaction of *p*-(dimethylamino)benzonitrile (DMABN) has been one of the most important examples of its type since Lippert et al.[1] first reported the dual fluorescence behavior in polar solvents. The twisted intramolecular charge transfer (TICT) model was proposed by Grabowski et al.[2] and Rettig,[3] which suggests a CT conformation where the dimethylamino (DMA) group undergoes a twist of 90° with respect to the benzonitrile moiety, allowing for the S_2/S_1 inversion. More recently, Zachariasse et al.[4] have developed the planar intramolecular charge transfer (PICT) model, which assumes that the CT state is nearly planar and the DMA inversion motion is an important driving force for the polar S_2 state coming into play. Although both mechanisms assume intramolecular structural reorganization accompanied by charge separation, the molecular basis for the CT stabilization is still under controversial discussion.[5−8]

Another important aspect of this reaction concerns whether similar CT dynamics occur in solvated clusters that can be prepared in supersonic expansions. Such jet-cooled clusters are expected to provide insight into the microscopic ways in which the solvation influences the stability of the CT state. Furthermore, one can investigate how the CT stability is extrapolated to the bulk as the solvation strength is increased. Previous supersonic jet studies[9−12] showed red-shifted fluorescence behavior for clusters of methyl *p*-(dimethylamino)benzoate with few solvent molecules. In this case, the lowest excited precursor state is considered to be of CT character since the energetically close-lying S_2 state becomes accessible in small solvent clusters, presumably due to the stronger electron affinity of the methyl ester group.

Similar studies for DMABN clusters resulted in conflicting data. Kobayashi et al.[13] first reported fluorescence from 1:1 complexes of DMABN with water and trifluoromethane, but these complexes were found to exhibit no CT fluorescence. A similar result was obtained by Peng et al.[14] for the 1:1 complex with water. Gibson et al.[15] indicated that multiple solvation of DMABN with methanol results in a substantial decrease in the fluorescence quantum yield, suggesting the formation of a nonemissive CT state. Subsequently, Bernstein's group[16,17] measured size-selective $S_1 \leftarrow S_0$ spectra of DMABN complexes with polar solvents by means of resonant enhanced two-photon ionization (R2PI) spectroscopy. For the 1:1 complex with acetonitrile, they found two structural isomers, one of which appears to exhibit fluorescence extending to longer than 400 nm.[17] Howell et al.[18] showed dual fluorescence behavior for DMABN complexes with various solvents and suggested that the long-wavelength emissions are associated with DMABN dimer or its solvated complexes, i.e., $(DMABN)_2(solvent)_n$. Analogous dual fluorescence was observed for DMABN complexes with acetonitrile by Krauss et al.,[19] using dispersed fluorescence spectroscopy combined with mass analysis. Contrary to the result of Howell et al., they assigned the red-shifted component of the emission to CT fluorescence from 1:*n* clusters and claimed that the CT formation requires a minimum of five acetonitrile molecules solvated with DMABN.

In the present paper, we report fluorescence behavior of DMABN complexes with acetonitrile and water as a function of solvent size distribution. In water clusters, selective excitation of each cluster is possible for $n = 1-3$ due to the discrete nature of their excitation bands, enabling us to observe respective excited-state behavior separately. The result indicates that the fluorescence from $n = 3$ cluster shifts suddenly to the red when excited with small amounts of excess vibrational energy. This

* Corresponding author: e-mail saigusa@yokohama-cu.ac.jp.

10.1021/jp030037g CCC: $25.00
Published on Web 05/31/2003

excitation energy dependence suggests that the underlying dynamics is structural isomerization into CT, yet its extent is much less than in the bulk solution. In both water and acetonitrile clusters, the fluorescence spectra for larger cluster sizes of $n = 10-20$ are found to be only slightly red-shifted with respect to those of the smaller sizes and do not converge to the bulk limit. The absence of characteristic CT emissions in the larger solvated clusters is explained by assuming that structural changes leading to CT are hindered by solvent cage effects.

Experimental Section

Spectroscopic techniques of R2PI, fluorescence excitation, and dispersed fluorescence employed in this work have been described previously.[20,21] In the present case, DMABN was heated to 380 K, seeded into 4 atm of He, and expanded in a vacuum chamber through a 0.25 mm orifice of a pulsed valve. However, the nozzle temperature was kept at ≈340 K in order to prevent the formation of homogeneous clusters of DMABN since they are known to give rise to interfering *excimer* fluorescence at >400 nm.[22] Solvent vapor (water or acetonitrile) was introduced by passing part of the helium carrier gas through a solvent reservoir and mixed with the sample vapor. The partial pressure of the solvent was controlled by varying the reservoir temperature and the mixing ratio.

The resulting cluster beam was irradiated at 10 mm downstream with the frequency-doubled output of a YAG-pumped dye laser (Continuum PL8000/ND6000/UVT-1). To obtain fluorescence excitation spectra, emissions were collected by a glass filter (UV34, UV35, LF399, or Y44) and detected with a PMT tube, while a 0.32-m monochromator (Jobin-Yvon HR320 with a 1200 lines/mm grating blazed at 330 nm) was used to obtain disperse fluorescence spectra. The sensitivity of this detection system was not corrected, but its spectral response was found to be ≈50% at 470 nm with respect to that at the blaze wavelength. Fluorescence spectra of DMABN in bulk solution were measured by placing the sample inside the vacuum chamber and exciting with the same laser system.

For recording R2PI spectra of respective cluster sizes, the molecular beam was skimmed with a 2.0-mm diameter skimmer placed at a distance of 20 mm from the nozzle and introduced in a second differentially pumped chamber. At 90 mm downstream of the nozzle, the skimmed beam was crossed by a portion of the UV laser beam. Ions produced via one-color R2PI were mass-analyzed by a Wiley−McLaren-type linear time-of-flight mass spectrometer and detected with a microchannel plate. The resulting mass spectrum enabled us to obtain information on the cluster size distribution in a nozzle expansion and identify the species that contributes the corresponding dispersed fluorescence spectrum. However, the cluster size distributions in the mass and emission spectra could be substantially different from each other since they are affected by spatial separation of clusters of different sizes due to the so-called Mach number focusing (vertical to the jet axis)[22] and velocity slip effect (parallel to the jet axis).[23] To minimize these effects, the size and position of the laser beam were adjusted carefully so that the same portion of the molecular beam was probed via R2PI as in the fluorescence measurements.

Hole-burning spectroscopy was employed to identify spectral features appearing in fluorescence excitation spectra. In the pump−probe experiment, fluorescence depletion signal caused by pump laser irradiation was measured by an alternative laser excitation method in which a spectral hole created by the pump laser at 5 Hz was probed by a second YAG-pumped dye laser (Continuum Surelite I/Spectra Physics PDL-1) at 10 Hz. The fluorescence signals with and without the pump laser irradiation were fed into a boxcar integrator and processed in a baseline subtraction mode.

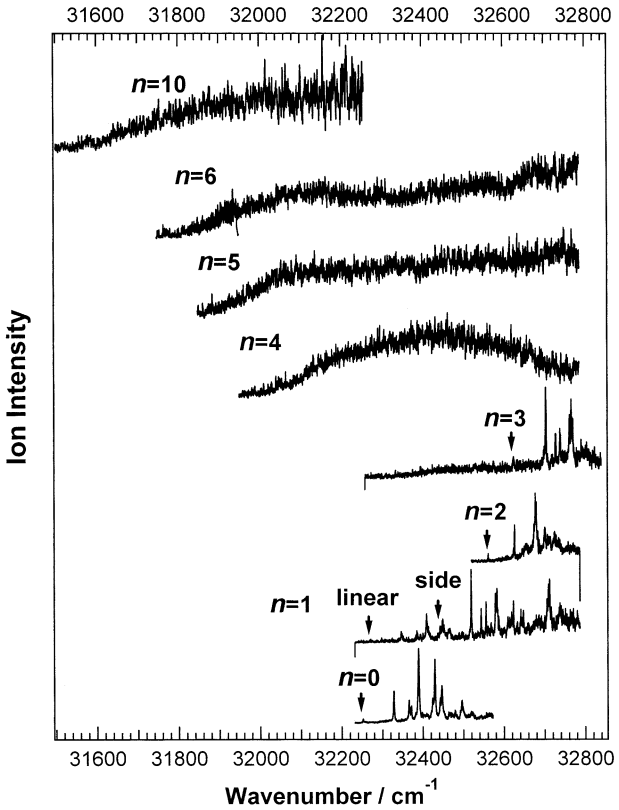

Figure 1. R2PI spectra of DMABN$(H_2O)_n$ clusters covering the S_1 electronic origin region of the DMABN chromophore. All spectra were measured at a nozzle temperature of ≈340 K and a He backing pressure of 4 atm. The S_1 origins of the DMABN monomer ($n = 0$) and clusters of $n = 1-3$ are indicated by arrows.

Results

A. Water Clusters. The R2PI spectra of DMABN$(H_2O)_n$ clusters covering the S_1 electronic origin region of the DMABN chromophore are shown in Figure 1. They agree well with those reported by Shang and Bernstein.[17] The $n = 1-3$ spectra are blue-shifted with respect to that of bare DMABN. The low-frequency spectral structures are similar to those of the bare molecule, indicating that the solvents are interacting with the benzonitrile moiety rather than the DMA group. It should also be noted that two structural isomers exist for the $n = 1$ cluster. The respective origins are shifted +19 and 190 cm^{-1} from that of the bare molecule. A theoretical calculation[24] suggests that the less blue-shifted isomer is assigned to a *linear* structure with one hydrogen of the water bonded to the cyano nitrogen. The other isomer is calculated to possess a *side* structure with the water molecule attached to both the C≡N group and the aromatic ring. In contrast, larger clusters of $n \geq 4$ give rise to broad, red-shifted spectra.

Figure 2 compares the R2PI spectra for $n = 1-3$ with an expanded scale. The general feature of the $n = 2$ spectrum, with its origin at +310 cm^{-1} from the bare molecule, resembles closely that of the $n = 1$ *linear* isomer. The $n = 3$ spectrum gives rise to its origin band shifted +377 cm^{-1} with respect to the bare molecule. It shows low-frequency features that are similar to those of the *side* isomer of $n = 1$. These spectral similarities suggest that in both $n = 2$ and $n = 3$ clusters the

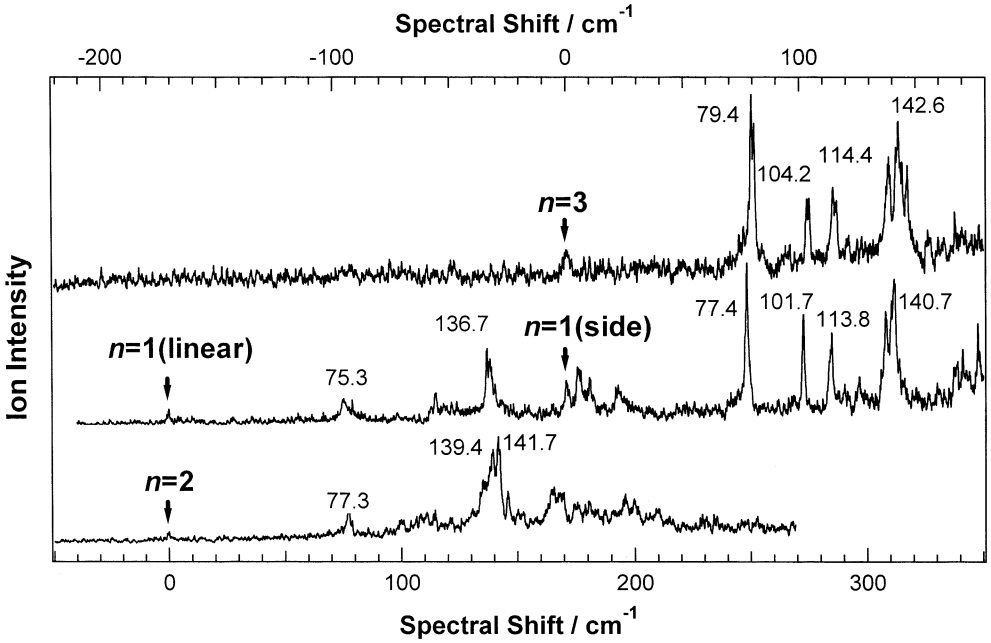

Figure 2. Expanded view of the R2PI spectra DMABN$(H_2O)_n$ clusters for $n = 1-3$ shown in Figure 1. The spectra of the clusters of $n = 1$ (*side* isomer) and $n = 3$ are positioned along the top axis with their origins aligned, while those of the $n = 1$ (*linear* isomer) and $n = 2$ clusters are shown similarly along the bottom axis.

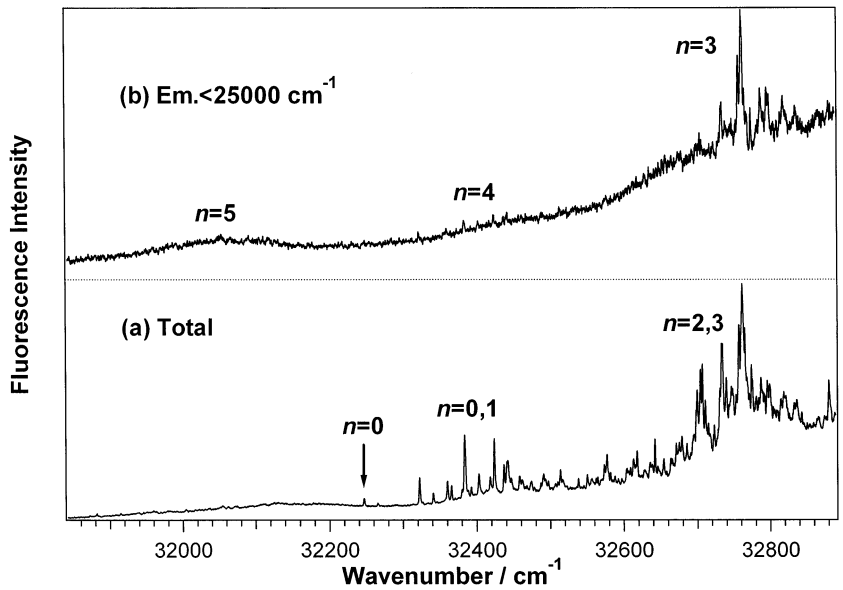

Figure 3. Fluorescence excitation spectra of DMABN$(H_2O)_n$ clusters in the vicinity of the bare molecule origin obtained by detecting (a) total fluorescence and (b) red-shifted fluorescence with a filter (50% transmission at ≈25 000 cm^{-1}). The nozzle expansion condition is the same as used to obtain spectra E in Figure 6. The arrow indicates the origin of the bare molecule at 32 247 cm^{-1}.

water molecules aggregate together and they are coordinated to the respective bonding sites of the C≡N group.

The fluorescence excitation spectra of DMABN$(H_2O)_n$ clusters in the vicinity of the bare molecule origin are shown in Figure 3. The spectrum in part a is obtained by probing total fluorescence signals reveals well-resolved features that correspond to the bare molecule and clusters of $n = 1-3$. When the fluorescence is filtered and its red-shifted portion (<25 000 cm^{-1}) is probed, most resolved features are nearly suppressed and broad excitation bands dominate in the entire energy region, as shown in part b of Figure 3. On the basis of comparison with the R2PI spectra (Figure 1), the broad features around 32 000 and 32 400 cm^{-1} can be associated primarily with those of $n = 5$ and $n = 4$, respectively. It should also be noted that prominent peaks which may be assigned to some of the $n = 3$ are observed at 32 750−32 800 cm^{-1} in the spectrum of part b.

A 200 cm^{-1} segment of the fluorescence excitation spectrum of the red-shifted component (part b in Figure 3) is shown in part a of Figure 4. Comparison with the R2PI spectrum of the $n = 3$ cluster (part b) reveals that the sharp spectral features observed around 143 cm^{-1} in the filtered fluorescence excitation spectrum correspond well to those of the $n = 3$ cluster. However, peaks corresponding to the energy features of $n = 3$ below 104 cm^{-1} are absent in the top spectrum. To identify the origin of these prominent features, we have employed hole-burning spectroscopy with probing the red-shifted fluorescence. The result is shown in part c of Figure 4, which was obtained by setting the probe laser to the 143 cm^{-1} peak (marked by an

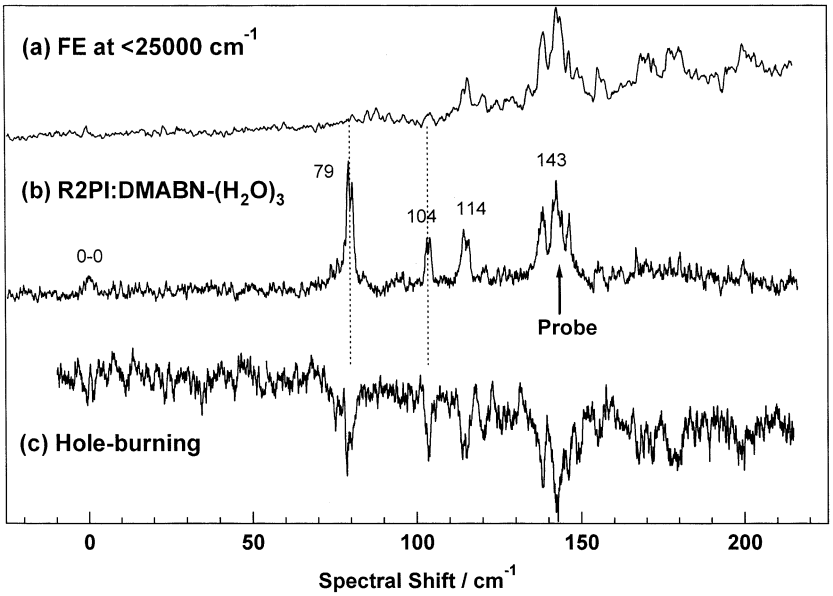

Figure 4. A 200 cm^{-1} segment of the origin region of the $n = 3$ cluster observed by (a) filtered fluorescence excitation at $<25\,000$ cm^{-1} (Figure 3b), (b) R2PI, and (c) hole-burning with fluorescence detection at $<25\,000$ cm^{-1}. The spectral shift is relative to the origin of the $n = 3$ cluster at 32 624 cm^{-1}. In the hole-burning measurement, the probe laser frequency was set at the 143 cm^{-1} peak of the $n = 3$ cluster (marked by the arrow in part b).

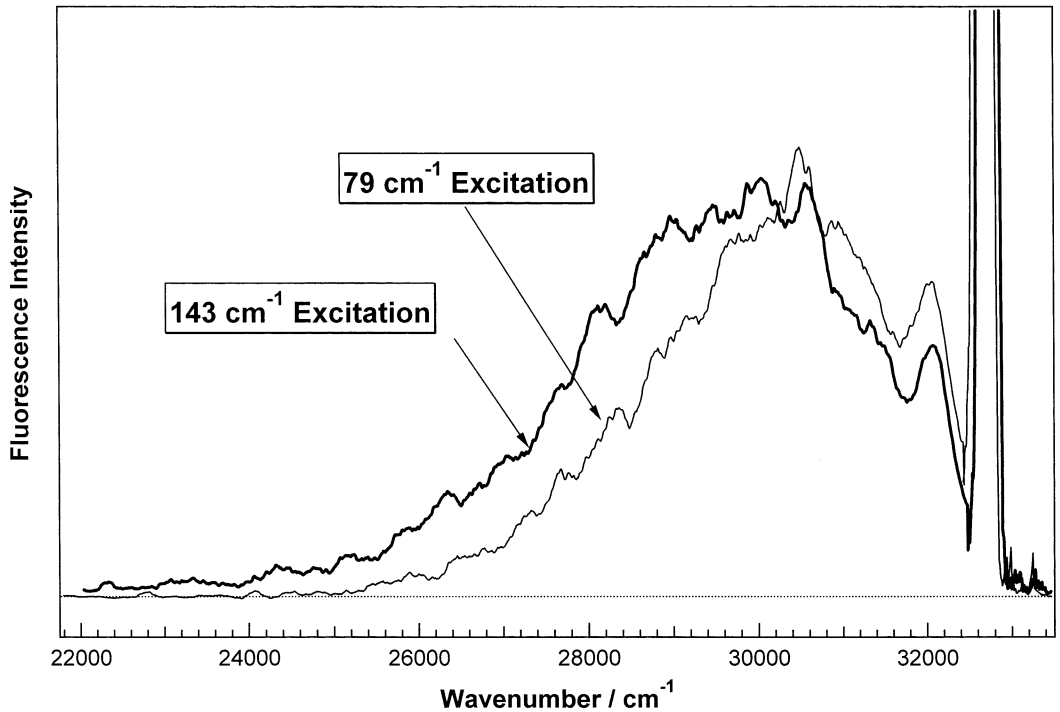

Figure 5. Dispersed fluorescence spectra obtained following excitation of the $n = 3$ cluster at 79 and 143 cm^{-1}. The corresponding cluster size distributions are shown in mass spectra C and D of Figure 6. The spectral resolution was $\approx$200 cm^{-1}. The highest energy feature in each spectrum is due to scattered laser light.

arrow in the R2PI spectrum) and detecting red-shifted fluorescence at $<25\,000$ cm^{-1}, while the pump laser was scanned over the energy region of the $n = 3$ cluster. It clearly shows the lower energy features at 79 and 104 cm^{-1}, which correspond well to those of $n = 3$, and indicates that the prominent features in the fluorescence excitation spectrum are associated with this cluster. This implies that the $n = 3$ fluorescence shifts suddenly to the red when excited with a small amount of excess energy. The observation apparently disagrees with a previous result obtained by Gibson et al.[15] They failed to detect fluorescence from $DMABN(H_2O)_n$ clusters of $n \geq 2$ and suggested that in these clusters water molecules interact with the DMA group, thus resulting in CT formation.

The dispersed fluorescence spectra of the $n = 3$ cluster obtained following excitation at 79 and 143 cm^{-1} are shown in Figure 5. It is evident that the 143 cm^{-1} fluorescence is substantially red-shifted with respect to that of the 79 cm^{-1} excitation. The distinct red shift, which is consistent with the results for $DMABN(acetonitrile)_n$ clusters described below, indicates that it undergoes structural changes upon excitation.

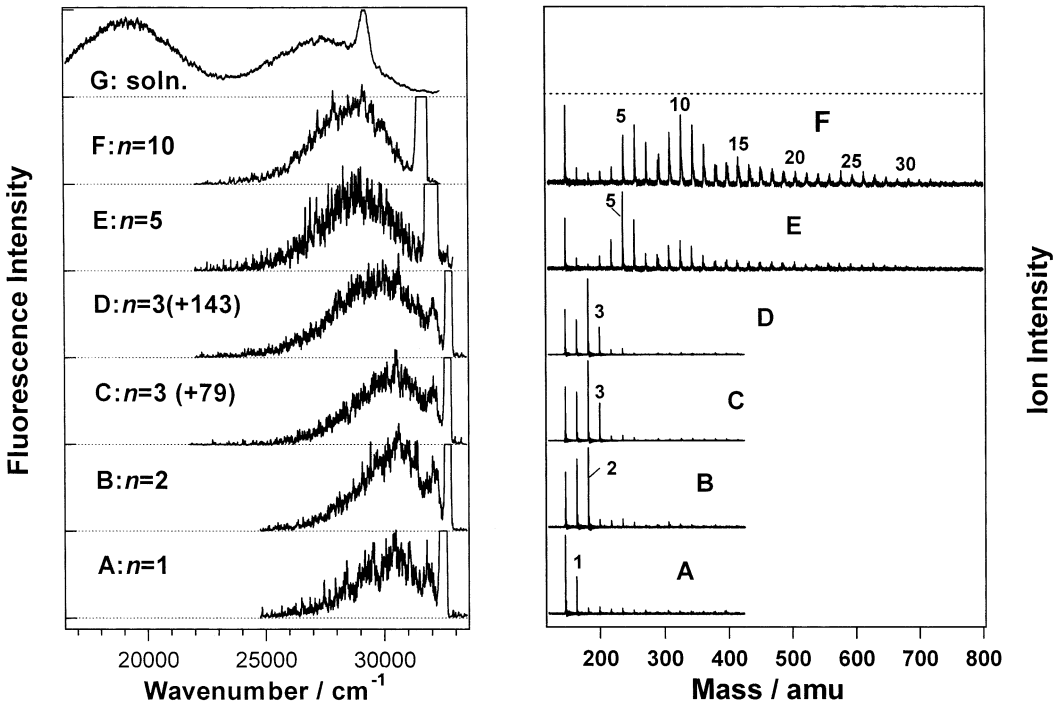

Figure 6. Dispersed fluorescence spectra for different DMABN$(H_2O)_n$ cluster distributions (left panels). The corresponding mass spectra obtained under the same nozzle expansion conditions as employed for the emission spectra are shown in the right panels. Cluster spectra A−F were measured by exciting the most prominent features in the respective R2PI spectra in Figure 1. The $n = 3$ spectra C and D correspond to those obtained at 79 and 143 cm^{-1} (shown in Figure 5). Dual fluorescence of DMABN in bulk water (298 K, 5×10^{-5} M), obtained with the same excitation and detection system as employed for collecting the cluster spectra, is shown in spectrum G. The spectral resolution was ≈200 cm^{-1} for A−D and ≈400 cm^{-1} for E−G. The truncated feature in spectra A−F is due to scattered laser light, while the sharp feature at ≈29 000 cm^{-1} in bulk spectrum G arises from Raman scattering.

The dynamical behavior is associated with the occurrence of CT, although its extent appears to be significantly less than in solution.

Figure 6 shows the dispersed fluorescence spectra for different DMABN$(H_2O)_n$ cluster distributions. The time-of-flight mass spectra obtained under the same nozzle expansion conditions as employed for the emission spectra are shown in the right panels. The excitation energy of each spectrum was set at the prominent feature appearing in the corresponding R2PI spectrum in Figure 1. Fluorescence spectra C and D are those for the $n = 3$ cluster obtained following excitation at 79 and 143 cm^{-1} (shown in Figure 5). Spectrum F is taken by exciting at 31 750 cm^{-1} for the largest cluster distribution where clusters of $n \approx 10$ are abundant and larger clusters of $n \geq 20$ are noticeable in the mass spectrum. The emission appears to be red-shifted only slightly with respect to the smaller cluster case (spectrum A). It is highly unlikely that upon further increase in the cluster size distribution the fluorescence spectra converge to the CT emission in bulk water (spectrum G), which shows a maximum at ≈19 000 cm^{-1}. Therefore, we conclude that the CT dynamics in these jet-cooled clusters and room-temperature bulk are substantially different from each other. As discussed later, this difference is associated with the low internal temperatures of the jet-cooled clusters.

B. Acetonitrile Clusters. Figure 7 shows the R2PI spectra for DMABN(acetonitrile)$_n$, $n = 1-10$, in the vicinity of the S_1 electronic origin of the bare DMABN (bottom spectrum). Sharp bands are seen only for the $n = 1$ cluster, which are blue-shifted with respect to the monomer. Shang and Bernstein[17] assigned these features to a structural isomer (*blue* isomer) with the acetonitrile molecule coordinated to the C≡N group. The $n = 1$ spectrum also reveals underlying broad bands that can be identified as another isomer (*red* isomer), as describe later. Large clusters of DMABN(acetonitrile)$_n$ have broad spectra similar to that of $n = 1$ but no resolved blue-shifted features. This situation contrasts with the case of the water clusters, where the excitation spectra vary significantly with cluster size (see Figure 1). The absence of any sharp spectral features associated with $n \geq 2$ clusters implies that size-selective excitation is not possible and a certain size range of clusters must be chosen to explore their excited-state dynamics.

Figure 8 shows the fluorescence spectra of DMABN-(acetonitrile)$_n$ clusters for different size distributions. The excitation was performed at 32 680 cm^{-1} (306 nm) where no resolved spectral feature of monomer or clusters can be seen in the R2PI spectra (Figure 7). The corresponding mass spectra are illustrated in the right panels. As the cluster size distribution is increased toward larger clusters, the emission maximum shifts to the red of the excitation. In the case of the largest observed cluster distribution H, where $n = 10-20$ clusters are discernible in the corresponding mass spectrum, its emission spectrum appears with an intensity maximum at ≈28 000 cm^{-1}. This emission is red-shifted only by ≈200 cm^{-1} with respect to the smallest cluster case (spectrum A). Therefore, analogous to the water clusters, the fluorescence spectra do not converge to the CT fluorescence peaking at ≈21 000 cm^{-1} observed in room-temperature solution (top spectrum in Figure 8). This result apparently disagrees with that reported by Krauss et al.[19] and will be discussed below.

A close examination of fluorescence spectra B and C in Figure 8 is shown in Figure 9, which reveals that there is a significant difference in their red shifts. The corresponding mass spectra indicate that $n = 3-5$ clusters are more abundant in spectrum C. The relatively small, albeit very distinct, red shift of fluorescence at $n = 3-5$ is consistent with the result for DMABN·$(H_2O)_n$ clusters. This indicates that CT stabilization

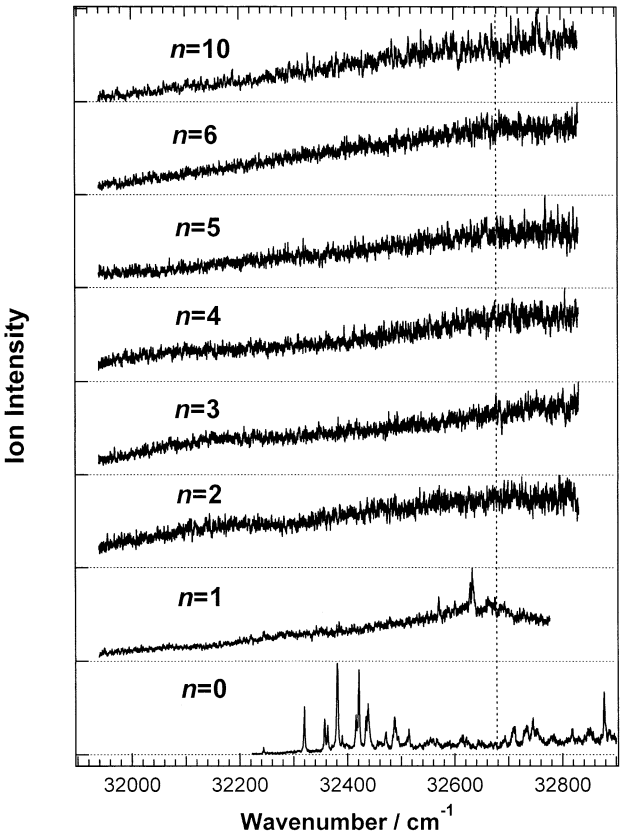

Figure 7. R2PI spectra for DMABN(acetonitrile)$_n$ in the vicinity of the S_1 electronic origin of the bare DMABN (bottom spectrum). The dotted line indicates the excitation energy used to measure the fluorescence spectra in Figure 8.

in DMABN(acetonitrile)$_n$ clusters also occurs weakly at $n = 3-5$, although its stability is significantly less than in solution. Further red shift is seen for larger cluster distributions, but only slightly with respect to the spectrum C. These observations suggest that the CT dynamics and subsequent relaxation in both clusters are substantially inhibited and the observed fluorescence may assigned as arising from an *unrelaxed* state of CT character.

Figure 10 compares the fluorescence excitation spectra in the energy region 30 800−32 800 cm^{-1} for the cluster distributions of A and E. The spectrum for the smaller size distribution A (part a) obtained by probing total fluorescence reveals congested spectral features corresponding to the *red* isomer of the 1:1 complex with its origin at ≈31 350 cm^{-1}. On the basis of its large red shift, Shang and Bernstein[17] suggested that this isomer possesses a geometry with the acetonitrile molecule over the aromatic ring with its dipole moment oriented antiparallel to that of DMABN. The spectrum in part b is obtained by scanning through the same energy region with a red filter (50% transmission at ≈25 000 cm^{-1}). It gives rise to little features due to the *red* 1:1 isomer, indicating no CT behavior for this isomer. The top panel (parts c and d) shows the corresponding spectra for the cluster distribution E. They are broad with no prominent features due to the monomer or the 1:1 complexes. Similar broad excitation spectra with no resolved features are observed for the larger cluster distributions F−H. This observation indicates that these species are nearly absent under these beam conditions, and the corresponding mass peaks appearing in the mass spectra E−H are predominantly due to fragmentation upon ionization.

Figure 11 shows the fluorescence spectra obtained for the cluster distributions of A and G. The bottom panel (parts a and b) compares the spectra obtained by exciting the *red* and *blue* isomers at the respective prominent peaks (shown in Figure 10a). The red shifts of the two spectra appear to be essentially identical, confirming the absence of CT behavior in both isomers. The spectra in parts c and d show those obtained for the cluster distribution G upon excitation at 31 250 and 32 680 cm^{-1} (indicated in Figure 10c). In this case, larger clusters of $n \geq 10$ are abundant, yet the fluorescence red shift is not significantly different from those for the smaller clusters. As explained in the Experimental Section, the absence of bulklike fluorescence cannot be due to the relatively low response function of the detection system in the lower energy range of <25 000 cm^{-1}. It is also evident that the fluorescence behavior is not dependent on the excitation energy explored in this study.

Discussion

The data presented above clearly show that there is a significant difference between the CT dynamics in cold clusters and in room-temperature bulk solution. Most evident is the absence of strongly red-shifted fluorescence in both water and acetonitrile clusters even for the largest cluster distribution of $n \geq 20$, which suggests that CT dynamics are slowed or impeded in these clusters. The result also shows evidence for the CT stabilization in water clusters where a sudden red shift in the fluorescence emission occurs at $n = 3$ upon excitation with a small amount of excess energy. Although its spectral shift is found to be much smaller than in bulk water, this threshold behavior is assigned to the occurrence of CT. These cluster-specific behaviors are discussed in terms of solvent cage effects associated with the low cluster internal energy.

A. Structure and CT Dynamics of Water Clusters. The R2PI spectra of DMABN(H$_2$O)$_n$ clusters for $n = 1-3$ are found to be blue-shifted and reveal low-frequency activity similar to the bare molecule, consistent with the results of Shang and Bernstein.[17] This behavior contrasts with water clusters of 4-aminobenzonitrile (ABN) where the first water molecule can hydrogen-bond to one of the hydrogen atoms of the amino group, giving rise to a red-shifted spectrum.[25,26] The difference in the bonding site between DMABN and ABN has been explained satisfactorily by a recent ab initio calculation performed at the MP2 level.[24] The result indicates that such structure is unstable for DMABN(H$_2$O)$_1$ due to the low atomic charge on the methyl hydrogens with respect to the amino hydrogens. The 1:1 complex reveals two origin bands that are blue-shifted by 19 and 190 cm^{-1} from the monomer. The latter isomer corresponds well to that for ABN(H$_2$O)$_1$ (194 cm^{-1}) and is identified as the *side* structure having the water molecule attached to both the cyano nitrogen and the aromatic ring. The 19 cm^{-1} isomer has no correspondence in ABN(H$_2$O)$_1$, which can be assigned to the *linear* isomer with the water hydrogen linearly bonded to the cyano nitrogen.

As illustrated in Figure 2, the 1:2 complex spectrum shows a low-frequency activity which resembles that of the *linear* isomer of the 1:1 complex. Therefore, it is suggested to have a structure in which the second water hydrogen-bonds to the first one of the *linear* isomer. Conversely, the R2PI spectrum of the 1:3 complex is analogous to that of the 1:1 complex having the *side* structure. This behavior could be rationalized by a structure with the additional water molecules hydrogen-bonded to the first one of the *side* isomer of the 1:1 complex. Previous supersonic jet studies showed no red-shifted fluorescence behavior for the bare DMABN molecule or the 1:1 complex with water. Kobayashi et al.[13] observed no fluorescence from complexes of 1:2 or higher stoichiometry and suggested that their absorption coefficients are very low. Gibson et al.[15] reported that multiple

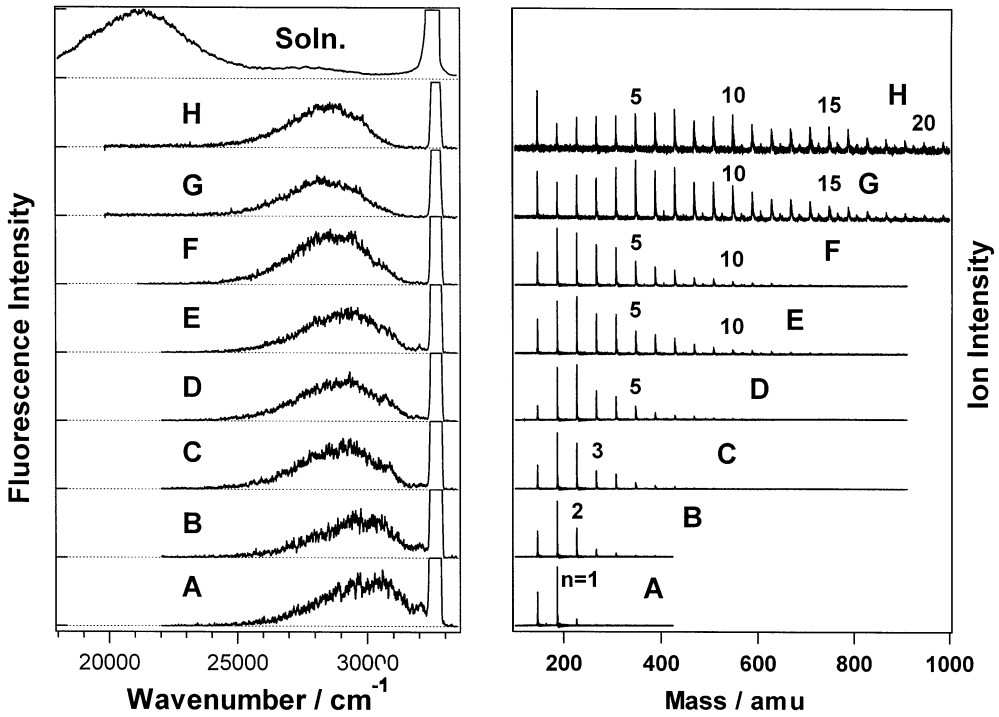

Figure 8. Fluorescence spectra of DMABN(acetonitrile)$_n$ clusters for different cluster distributions (spectra A−H in left panels). The mass spectra obtained under the same conditions as employed for the emission spectra are shown in the right panels. Dual fluorescence of DMABN in acetonitrile solution (298 K, 5×10^{-5} M) obtained with the same excitation and detection setup is shown in the top panel. All spectra are scaled to the same height. The monochromator resolution was ≈200 cm^{-1}. The highest energy feature (at 32 680 cm^{-1}) in each emission spectrum is due to scattered laser light.

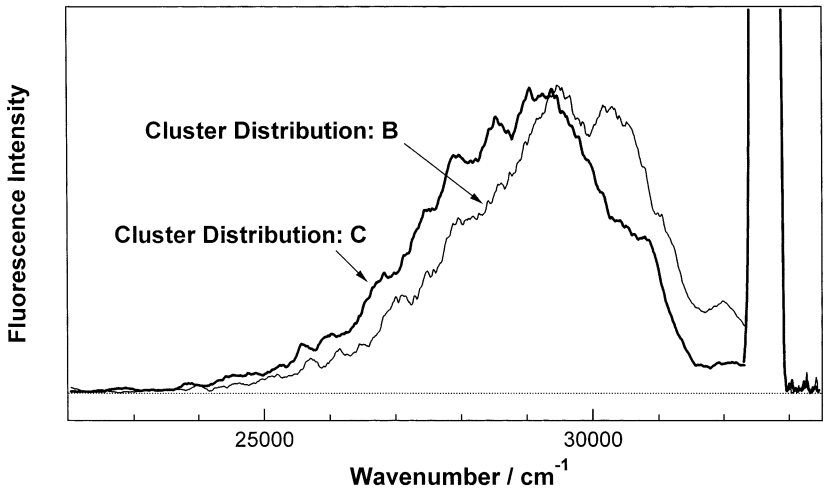

Figure 9. Expanded view of the fluorescence spectra of DMABN(acetonitrile)$_n$ for the cluster distributions of B and C shown in Figure 8.

solvation of DMABN with protic molecules (e.g., water and methanol) results in a substantial decrease in the fluorescence quantum yield, from which the formation of a non-emissive CT state was inferred. Contrary to these results, we have observed that the 1:1 and 1:2 complexes give rise to fluorescence emissions which are similar to that of the bare molecule, giving no indication of CT stabilization. This is consistent with the result of Kobayashi et al.[13]

The fluorescence spectrum of 1:3 complex shows a sudden red shift in the low excess energy region. The prominent fluorescence shift indicates that the complex undergoes structural isomerization following S_1 excitation, implicating the occurrence of CT. However, the spectral shift, which may be associated with the extent of CT stabilization, is much smaller than in bulk water. This difference can be rationalized on the basis of an assumption that the addition of three water molecules is just enough to induce S_2/S_1 inversion but insufficient to stabilize the CT state as in bulk water. Therefore, we conclude that the threshold cluster size for CT is $n = 3$ and there is a very low energy barrier to the CT formation. Subsequent solvation results in red shifts and broadening of the R2PI spectra (Figure 1). The absence of resolved low-frequency structure for $n \geq 4$ suggests that the additional water molecules are attached to the DMA group and the CT state is located lower than in the $n = 3$ cluster. Nevertheless, the red shifts of the fluorescence spectra for the larger cluster distributions (spectra E and F in Figure 6) appear to saturate. Although they are red-shifted compared with the spectra for the smaller cluster cases A−D, their magnitudes are significantly less than the CT emission in bulk water (spectrum G) and rather similar to the LE emission.

These considerations suggest that the major factors controlling the excited-state CT in the solvent clusters are the solvent

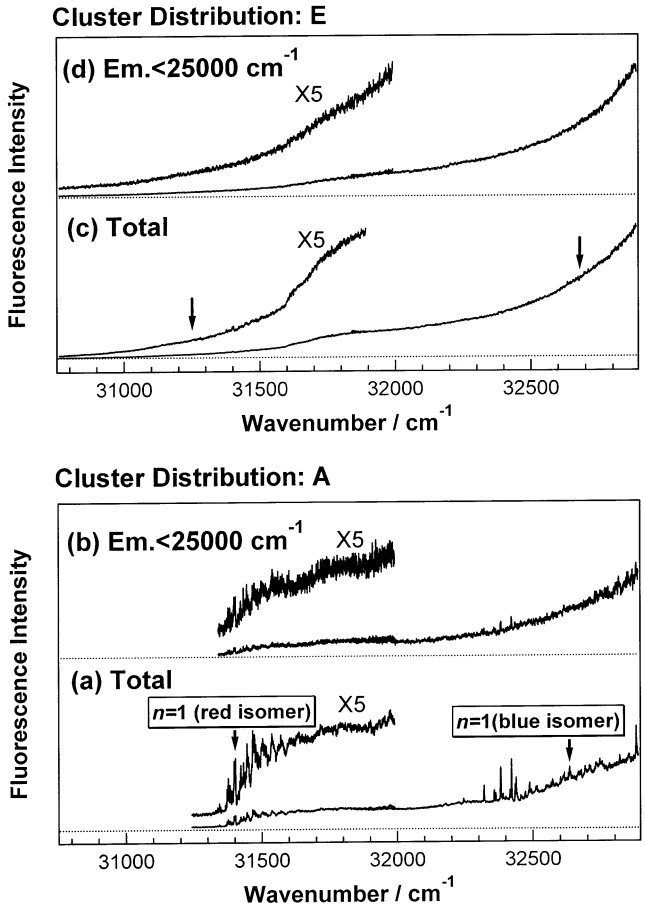

Figure 10. Fluorescence excitation spectra of DMABN(acetonitrile)$_n$ in the energy region 30 800−32 800 cm^{-1} for the cluster distributions of A (bottom panel) and E (top panel). The lower and upper spectra in each panel are obtained by probing total fluorescence and red-shifted fluorescence at <25 000 cm^{-1} (>400 nm), respectively. The arrows indicate the excitation energies of the emission spectra depicted in Figure 11.

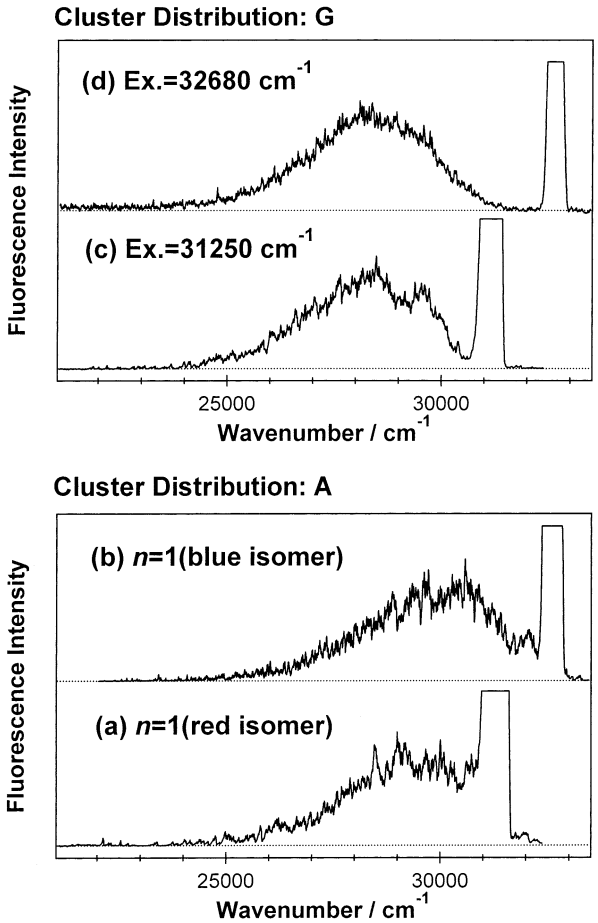

Figure 11. Fluorescence spectra of DMABN(acetonitrile)$_n$ for the cluster distributions of A (bottom panel) and G (top panel) obtained at two different excitation energies. The spectra for the size distribution A are obtained by exciting the prominent peaks corresponding to the *red* and *blue* isomers (marked by arrows in Figure 10a). The spectra for the cluster distribution G are obtained by exciting at 31 250 and 32 680 cm^{-1} (marked by arrows in Figure 10c). The spectral resolution was ≈400 cm^{-1} for all spectra. The truncated feature in each spectrum is due to scattered laser light.

polarity and rigidity. Small clusters of $n \leq 5$ are structurally less rigid and thus undergo rapid solvent reorganization upon excitation. In this case, the first factor prevails. The solvent polarity of these clusters is unknown (dielectric constant $\epsilon = 78.5$ for water at 293 K) but should be dependent greatly on the cluster size. With small numbers of solvent molecules, it is not sufficient to induce large CT stabilization of the solute. In larger clusters, the large solvent polarity may induce inversion of the initially excited S_1 state and the S_2 state of CT character. Thus, the rigidity of the surrounding solvent molecules is decisive in enabling the level inversion via relaxation and reorganization of surrounding water molecules. If solvent reorganization takes place, then the solute undergoes conformational changes leading to CT as in bulk solution.

Local solvent structure may also play a role in inducing such level inversion and CT stabilization. In the case of benzene-$(H_2O)_n$ clusters of $n \leq 5$, all solvent molecules were found to aggregate together on the same side of the benzene ring and interact with the solute.[27] Larger water clusters of DMABN may have similar local structures, while those of acetonitrile clusters are likely to surround the solute and form a cagelike solvent structure. In this case, the effective solvent polarity in water clusters could be much less than in acetonitrile ($\epsilon = 37.5$ for acetonitrile at 293 K). Such structural factors may account for the observation that the fluorescence spectrum of the largest observed water clusters (cluster distribution F in Figure 6) appears to be less red-shifted with respect to that of acetonitrile clusters of similar sizes (cluster distribution H in Figure 8). However, it should be noted that the fluorescence spectra of the large acetonitrile clusters are not as strongly red-shifted as in bulk solution (top spectrum in Figure 8). This suggested that the local structural factor is not dominant and the CT stabilization is largely controlled by the solvent rigidity.

Similar large differences between the excited-state dynamics in clusters and liquid phase are observed for proton-transfer reaction of naphthols. Knochenmuss and Leutwyler[28] showed that proton transfer in 1-naphthol·water clusters occurs in larger clusters of ≈25 water molecules. However, the extent of proton transfer, which is manifested by a red shift in the fluorescence, was found to be less than in bulk water. This behavior was explained on the basis of the gas-phase proton affinity of the solvent cluster and the solvent reorganization. Furthermore, Knochenmuss and Smith[29] demonstrated that the extent of proton transfer in these clusters varies with the cluster internal energy and suggested that the dynamics is controlled by the rate of solvent relaxation.

B. Structure and CT Dynamics of Acetonitrile Clusters. The DMABN(acetonitrile)$_1$ shows two structural isomers. Shang and Bernstein[17] assigned the *blue* isomer to a structure in which the acetonitrile molecule is coordinated to the CN moiety and the *red* one to that with the solvent located over the aromatic

ring. They also suggested CT stabilization for the latter isomer. However, we have observed that the two structural isomers show similar fluorescence spectra (Figure 11a,b), indicative of no excited-state dynamics in either isomer. For larger clusters of $n \geq 2$, CT dynamics have been explored as a function of cluster size distribution. The fluorescence spectrum for the cluster distribution C (shown in Figure 9) is red-shifted with respect to that for the distribution B. The difference can be attributed to the clusters of $n = 3-5$, which are more abundant in the distribution C. This threshold CT behavior agrees with the result for DMABN$(H_2O)_n$ clusters in which CT occurs for $n \geq 3$ clusters.

Further red shift of fluorescence is seen in going from the cluster distribution D to H, but only slightly with respect to spectrum C. This cluster behavior is also consistent with the results for the water clusters described above and associated with the low internal temperatures of the clusters generated from jet expansions. As the cluster size increases, the DMABN solute may be completely surrounded by solvent molecules. Since the S_2 excited state is believed to be quite polar relative to the initially excited S_1 state, its stabilization energy should be greatly altered by solvent cage effects. This implies that there exist activation barriers along the CT stabilization coordinate, which is evident in the water cluster of $n = 3$. In this case, structural changes may occur within the solvent cage to produce an *unrelaxed* CT state that correlates with the S_2 state, and the observed fluorescence is assigned as arising from this state. Based on the absence of bulklike CT stabilization in these clusters, an inference can be made that the CT dynamics is accompanied by substantial changes in the conformation of the solute like those implicated in the TICT model,[2,3] i.e., twisting of the DMA group with respect to the benzonitrile moiety.

In contrast to our observation, Howell et al.[18] reported dual fluorescence in DMABN(acetonitrile)$_n$ clusters. They assigned the redder component of the fluorescence centered at 414 nm ($\approx$24 150 cm^{-1}) as arising from a DMABN dimer or its solvated clusters, on the basis of the nozzle temperature dependence of its intensity. Similar greatly red-shifted fluorescence was observed at 425 nm ($\approx$23 500 cm^{-1}) by Krauss et al.[19] for a cluster distribution where clusters of $n \geq 5$ are noticeable. The red-shifted component was obtained through excitation at 306.24 nm (corresponding to the most prominent feature of the $n = 1$ cluster in Figure 7) and attributed to CT fluorescence from clusters of $n \geq 5$. It should be noted that the general feature of their cluster distribution exhibiting the dual fluorescence resembles that of spectrum C in Figure 1 (obtained at 306 nm). Although we suggest that clusters involving DMABN dimer are responsible for the appearance of the dual fluorescence at this excitation energy, a more detailed investigation is needed for explaining the apparently different observations.

The solvent rigidity scenario that the dynamics in the cold clusters is kinetically limited by a solvent cage is consistent with a recent result obtained for DMABN in an acetonitrile matrix by Suzuka et al.[30] They showed that its CT emission vanishes abruptly just below 200 K and phosphorescence of DMABN appears in this crystal. This behavior was explained by a distinct phase transition occurring from the monoclinic to orthorhombic phase of acetonitrile in this temperature range.[31] The low-temperature phase has a more packed structure with eight molecules in a unit cell, which presumably suppresses the CT dynamics. The importance of such solvent cage effects also agrees with the results for the water clusters described above.

These considerations suggest that bulklike CT dynamics may be observed in larger clusters upon increasing the cluster temperature. Consistent with this expectation, we have recently demonstrated that dual fluorescence behavior can be observed in the DMABN$(CH_3CN)_n$ clusters upon increasing the excitation energy of the DMABN solute.[21] The red-shifted component, termed *relaxed* CT fluorescence, has been found to grow in relative intensity as the excess energy is increased with respect to the S_1 origin. When an excess amount of energy is deposited on the solute, it will flow rapidly into low-frequency solute−solvent modes, thereby enabling reorientation of the solvent molecules in the proximity of the solute. This in turn facilitates geometrical changes of the solute leading to CT while evaporating solvent molecule(s), which are presumably located on the exterior of the cluster. Thus the dual fluorescence behavior appears to be strongly dependent on the cluster size distribution. For the cluster distribution E in Figure 8, where moderate-size clusters $n = 5-10$ are abundant, a threshold excess energy of 2500−3000 cm^{-1} is required for facilitating the CT relaxation.[21]

In contrast to the acetonitrile clusters, little bulklike CT fluorescence has been observed for DMABN·water clusters when excited over the same excess energy range.[21] The lack of significant CT stabilization in water clusters could be associated with solvent reorganization, which must involve breaking of hydrogen bonds. The structural rigidity scenario suggests that more excess energy is required for activation of CT in water clusters. Another possible factor for the difference between the water and acetonitrile clusters is the local solvent structure, as discussed above. Thus the water clusters are expected to dissociate together upon excitation to produce smaller clusters having a few water molecules, thus explaining the absence of large CT stabilization.

Conclusions

R2PI, fluorescence excitation, and dispersed fluorescence spectra of DMABN clusters solvated with water and acetonitrile have been measured to investigate their structure and excited-state CT dynamics as a function of the solvation number. In either solvent case, no dynamical behavior is observed for small clusters of $n \leq 2$. The water cluster of $n = 3$ gives rise to a distinct red shift of fluorescence when excited with excess energies of $\approx$100 cm^{-1} above its S_1 origin. The excitation energy dependence is assigned to an activation of CT stabilization in this cluster. A similar threshold CT behavior is found for acetonitrile clusters. The extent of CT appears to saturate at cluster sizes of $n \approx 10$ in both solvents and does not converge to the bulk limit. The observation suggests that the CT stabilization in larger clusters is impeded by solvent cage effects associated with the low cluster temperature, thus requiring substantial activation. These cluster CT dynamics are expected to be gradually extrapolated to those occurring in bulk solution upon increasing cluster temperatures and facilitating solvent reorganization. We are currently attempting to promote such CT activation in large clusters via direct excitation of solvent molecules using IR lasers.

Acknowledgment. This work was supported in part by the Sumitomo Foundation for Basic Research. We are grateful to Professors I. Suzuka and H. Sekiya for communicating their results prior to publication and to Professor T. Zwier for suggesting the use of hole-burning spectroscopy.

References and Notes

(1) Lippert, E.; Lüder, W.; Boos, H. In *Advances in Molecular Spectroscopy*; Mangini, A., Ed.; Pergamon: Oxford, U.K., 1962; p 443.

(2) Grabowski, Z. R.; Rotkiewicz, K.; Siemiarczuk, A.; Cowley, D. J.; Baumann, W. *Nouv. J. Chim.* **1979**, *3*, 443.

(3) Rettig, W. *Angew. Chem., Int. Ed. Engl.* **1986**, *25*, 971.

(4) Zachariasse, K. A.; von der Haar, Th.; Hebeker, A.; Leinhos, U.; Kühnle, W. *Pure Appl. Chem.* **1993**, *65*, 1745.
(5) Rettig, W.; Bliss, B.; Dirnberger, K. *Chem. Phys. Lett.* **1999**, *305*, 8.
(6) Zachariasse, K. A. *Chem. Phys. Lett.* **2000**, *320*, 8.
(7) Kwok, W. M.; Ma, C.; Matousek, P.; Parker, A. W.; Phillips, D.; Toner, W. T.; Towrie, M.; Umapahty, S. *J. Phys. Chem. A* **2001**, *105*, 984.
(8) Okamoto, H.; Inishi. H.; Nakamura, Y.; Kohtani, S.; Nakagaki, R. *J. Phys. Chem. A* **2001**, *105*, 4182.
(9) Weersink, R. A.; Wallace, S. C. *J. Phys. Chem.* **1994**, *98*, 10710.
(10) Dedonder-Lardeux, C.; Jouvet, C.; Martrenchard, S.; Solgardi, D. McCombie, J.; Howells, B. D.; Palmer, T. F.; Subaric-Leitis, A.; Monte, C.; Rettig, W.; Zimmermann, P. *Chem Phys.* **1995**, *191*, 271.
(11) Grégoire, G.; Dimicoli, I.; Mons, M.; Dedonder-Lardeux, C.; Jouvet, C.; Martrenchard, S.; Solgardi, D. *J. Phys. Chem. A* **1998**, *102*, 7896.
(12) Krauss, O.; Brutschy, B. *Chem. Phys. Lett.* **2001**, *350*, 427.
(13) Kobayashi, T.; Futakami, M.; Kajimoto, O. *Chem. Phys. Lett.* **1986**, *130*, 63.
(14) Peng, L. W.; Dantus, M.; Zewail, A. H.; Kemnitz, K.; Hicks, M.; Eisental, K. B. *J. Phys. Chem.* **1987**, *91*, 6162.
(15) Gibson, E. M.; Jones, A. C.; Phillips, D. *Chem. Phys. Lett.* **1987**, *136*, 454.
(16) Grassian, V. H.; Warren, J. A.; Bernstein, E. R.; Secor, H. V. *J. Chem. Phys.* **1989**, *90*, 3994.
(17) Shang, Q.; Bernstein, E. R. *J. Chem. Phys.* **1992**, *97*, 60.
(18) Howell, R.; Phillips, D.; Petek, H.; Yoshihara, K. *Chem. Phys.* **1994**, *188*, 303.
(19) Krauss, O.; Lommatzsch, U.; Lahmann, C.; Brutschy, B.; Rettig, W.; Herbich, J. *Phys. Chem. Chem. Phys.* **2001**, *3*, 74.
(20) Hirata, T.; Ikeda, H.; Saigusa, H. *J. Phys. Chem. A* **1999**, *103*, 1014.
(21) Saigusa, H.; Iwase, E.; Nishimura, M. *J. Phys. Chem. A* **2003**, *107*, 3759.
(22) Lommatzsch, U.; Gerlach, A.; Lahmann, C.; Brutschy, B. *J. Phys. Chem. A* **1998**, *102*, 6421.
(23) Droz, T.; Knochenmuss, R.; Leutwyler, S. *J. Chem. Phys.* **1990**, *93*, 4520.
(24) Mori, H.; Sekiya, H. Unpublished results.
(25) Sakota, K.; Yamamoto, N.; Ohashi, K.; Sekiya, H.; Saeki, M.; Ishiuchi. S.; Sakai, M.; Fujii, M. *Chem. Phys. Lett.* **2001**, *341*, 70.
(26) Alejandro, E.; Fernández, J. A.; Castaño, F. *Chem. Phys. Lett.* **2002**, *353*, 195.
(27) Garrett, A. W.; Zwier, T. S. *J. Chem. Phys.* **1992**, *96*, 3402.
(28) Knochenmuss, R.; Leutwyler, S. *J. Chem. Phys.* **1989**, *91*, 1268.
(29) Knochenmuss, R.; Smith. D. E. *J. Chem. Phys.* **1994**, *101*, 7327.
(30) Suzuka, I., et al. Unpublished results.
(31) Torrie, B. H.; Powell, B. M. *Mol. Phys.* **1992**, *75*, 613.